VABLJENO PREDAVANJE

Dave M. POTTS
Prof. Dr., FREng, CEng.

Imperial College, London

APPROPRIATE CONSTITUTIVE MODELS FOR GEOMATERIALS

KONSTITUTIVNI MODELI ZA MATERIALE V GEOTEHNIKI

Biografija

Prof.dr. Dave M. Potts
BSc PhD DSc FREng CEng FICE

Letnica rojstva: 1952

Izobrazba:

Kings College, London		
	BSc (1st Class)	1973
Cambridge University	PhD	1976
Imperial College, London	DSc	1996

Strokovna usposobljenost in izkušnje

Po končani diplomi na Kings Collegeu v Londonu se je profesor Potts ukvarjal z raziskovalnim delom na Univerzi v Cambridgeu. Raziskave so bile s področja porušitve plitvih predorov in so vsebovale obsežne eksperimentalne in analitične študije. Z univerze je šel k Raziskovalnim laboratorijem podjetja Shell v Rijswijk na Nizozemskem, kjer je delal na eksperimentalnih in teoretičnih problemih cikličnih obremenitev glin, na razvoju numeričnih metod za analizo obnašanja temeljenja težnostnih konstrukcij na obali, na napetostih naftnih rezervoarjev in na stabilnosti cevovodov v morju.

Od leta 1979 je profesor Potts član akademskega osebja na Imperial Collegeu, odgovoren za poučevanje uporabe analitičnih metod v geomehaniki ter projektiranje pobočij in zemljinskih podpornih konstrukcij, tako na dodiplomskem kot podiplomskem študiju. Trenutno je vodja oddelka za mehaniko tal. Profesor Potts je obsežno delal na razvoju analiz s pomočjo računalniških metod, zlasti z uporabo programov, ki zajemajo elasto plastične analize s končnimi elementi, za projektiranje dejanskih geotehničnih konstrukcij. Njegovo svetovalno delo je zajemalo projektiranje pilotov, vključno z nateznimi piloti za sidrane ploščadi, odzivi temeljev gravitacijskih ploščadi na ciklično obremenitev, podpornih konstrukcij različnih tipov, predorov po tehnologiji cut&cover, vrtanih predorov, kanalov pri pogrezanju zaradi rudarjenja, stabilnost nasipov na slabo nosilnih tleh, obnašanje konstrukcij iz armirane zemljine, napoved premikov tal v okolici globokih izkopov in vlogi stopnjujoče porušitve nasipov ter problemih vkopov v pobočjih.

Profesor Potts je svetoval nekaj naftnim podjetjem, svetovalcem in vladnemu laboratoriju za raziskave pri uporabi računskih metod in je v okviru oddelka za mehaniko tal na Imperial Colegeu ustvaril popolnoma opremljen računski laboratorij. Profesor Potts je avtor ali soavtor več kot 150 strokovnih publikacij in je bil nagrajen z medaljo Georgea Stephensona leta 1983, medaljo Coopers Hill War Memorial leta 1985, medaljo Telforda leta 1991, nagrado Telford leta 1997, nagrado Crampton leta 1998 in medaljo Telforda leta 1998, vse podeljene Zavoda za gradbeništvo (Institution of Civil Engineering). Skupaj z dr. Jardineom z Imperial Collegea je leta 1989 predstavil prvo BGS/geotehnično predavanje (BGS/Geotechnique) in je član Geotehnične svetovalne porote (Geotechnique Advisory Panel). Deloval je v raznih komitejih za Mednarodno združenje za mehaniko tal in temeljenje

(ISSMFE), Zavod za gradbeništvo (ICE), Zavod za konstrukcije (ISE) in Zavod za standardizacijo (BSI). Leta 2001 je postal član Kraljeve akademije inženirjev ter je v letu 2002 podal 42. Rankinovo predavanje.

Biography

Prof. Dave M. Potts
BSc PhD DSc FREng CEng FICE

Year of birth: 1952

Education:

Kings College, London		
	BSc (1st Class)	1973
Cambridge University	PhD	1976
Imperial College, London	DSc	1996

Professional Background and Experience

After graduation from Kings College, London, Professor Potts undertook research at Cambridge University into the collapse of shallow tunnels which involved extensive experimental and analytical studies. From Cambridge he went to the Shell Research Laboratories, Rijswijk, Holland where he worked on experimental and theoretical problems involved in the cyclic loading of clay, on the development of numerical methods for analysing the foundation behaviour of marine gravity structures, on the stresses in oil well casings, and on the stability of offshore pipelines.

Since 1979 Professor Potts has been a member of the academic staff at Imperial College, responsible for teaching the use of analytical methods in geomechanics and the design of slopes and earth retaining structures, both at undergraduate and postgraduate levels. He currently holds the position of head of the Soil Mechanics Section. Professor Potts has worked extensively on the development of computer methods of analysis and, more particularly, on the application of elasto-plastic finite element programs to the design of real geotechnical structures. His consulting work has been concerned with the design of piles, including tension piles for offshore anchored structures, the response of offshore gravity platform foundations to cyclic loading, retaining structures of various types, cut-and-cover tunnels, bored tunnels, culverts subject to mining subsidence, the stability of embankments on soft ground, the behaviour of reinforced earth structures, the prediction of ground movements around deep excavations and the role of progressive failure in embankment and cut slope problems.

Professor Potts has advised several oil companies, consultants and a government research laboratory on the use of computational methods, and has set up a fully equipped computational facility within the Soil Mechanics Section at Imperial College. Professor Potts has been author and co-author of more than 150 technical publications and was awarded the George Stephenson medal in 1983, the Coopers Hill War Memorial medal in 1985, the Telford Medal in 1991, a Telford Premium in 1997, the Crampton Prize in 1998 and the Telford Medal in 1998, all by the Institution of Civil Engineers. He presented the1st BGS/Geotechnique Lecture in 1989 jointly with Dr Jardine of Imperial College and has been a member of the Geotechnique Advisory Panel. He has served on various committees for the International Society of Soil Mechanics and Foundation Engineering, the Institution of Civil Engineers, the Institution of Structural Engineers, and the British Standards Institution. He was made a fellow of the Royal Academy of Engineers in 2001 and gave the 42nd Rankine Lecture in 2002.

APPROPRIATE CONSTITUTIVE MODELS FOR GEOMATERIALS

KONSTITUTIVNI MODELI ZA MATERIALE V GEOTEHNIKI

D.M. Potts

Department of Civil and Environmental Engineering, Imperial College, London, UK

POVZETEK

V geotehničnih analizah je eden od najpomembnejših sestavnih delov primerna izbira konstitutivnega modela, ki bo predstavil obnašanje zemljine. Obstaja mnogo takšnih modelov, vendar jih lahko samo nekaj zajame realno obnašanje zemljine na osnovi parametrov dobljenih iz standardnih terenskih preiskav. Bolj, ko je model, ki opisuje obnašanje zemljine natančen, večje je število parametrov, ki ta model definira. V prispevku so prikazane za nekatere tipe konstitutivnih odnosov sposobnosti njihovega napovedovanje realnega obnašanja. V ta namen je narejena primerjava med napovedmi obnašanja in rezultati terenskih meritev na praktičnih primerih.

Appropriate constitutive models for geomaterials

D.M. Potts
Department of Civil and Environmental Engineering, Imperial College, London, UK

ABSTRACT

One of the most important ingredients of any geotechnical analysis is the constitutive model used to represent soil behaviour. Many such models currently exist, but very few can describe all facets of real soil behaviour based on parameters which can be obtained from standard site investigation tests. The more accurate the model is at reproducing real soil behaviour, the greater is the number of input parameters required to define it. This paper reviews the ability of certain types of constitutive model to reproduce real behaviour. This is done by considering field cases in which predictions are compared with field measurements.

1 INTRODUCTION

The use of numerical analysis, such as the finite element method, when applied to geotechnical problems can be extremely complex. While in principle the method can be used to provide a solution to most of the problems that may arise, there are approximations which can lead to errors. These approximations can be classified into two groups. Firstly, there are approximations in the numerical method (i.e. finite element method) itself and secondly, there are approximations arising from the idealisations made by the user when reducing the real problem to a form which can be analysed (Potts & Zdravkovic, 1999).

Examples of the second group are the many potential errors which can be associated with a user's lack of 'in depth' understanding of the constitutive model employed to represent soil behaviour. There is a large number of constitutive models available. These range from very simple models (e.g. linear elastic) through to much more complex models which are rarely used in practice (e.g. MIT-E3 (Whittle, 1993)). When undertaking an analysis of any form it is important to consider which models are appropriate for the situation under consideration. It may be that under certain circumstances simple models are sufficient to obtain reasonable results, but for other types of problem a greater degree of sophistication is required.

This paper first identifies some of the main facets of soil behaviour by considering results from laboratory tests and then reviews several case histories in which the author has been involved. All of these have involved finite element analyses using the computer code ICFEP (Imperial College Finite Element Program), which has an extensive library of constitutive models (Potts & Zdravkovic, 1999). In the majority of cases the analysis were of the Class A type, being performed before the field measurements were made. Attention will be placed on the type of constitutive model employed and the ability of the analyses to predict the field behaviour.

2 REAL SOIL BEHAVIOUR

Soil behaviour is a complex subject and it is not possible to cover every aspect here. Consequently, only some of the most important issues are discussed.

2.1 Behaviour under one dimensional compression

The behaviour of clays under one dimensional compression is usually investigated in an oedometer. Results from tests on reconstituted Pappadai clay (Cotecchia, 1996) are shown in Figure 1, where the vertical effective stress, σ_v', is plotted against the void ratio, *e*. The soil sample has been subjected to compression with two cycles of unloading/reloading.

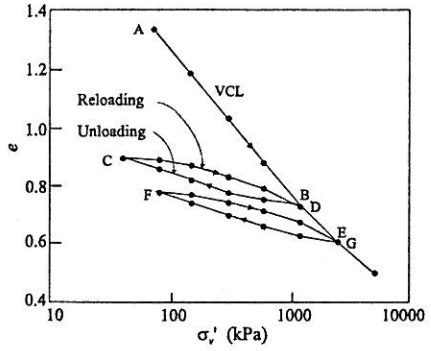

Figure 1: One-dimensional consolidation of Pappadai clay (Cotecchia, 1996)

In its initial condition, when placed in the oedometer, the reconstituted clay is in a normally consolidated state represented by point A in Figure 1. On loading (increasing σ_v') the sample compresses and its void ratio reduces travelling down the virgin consolidation line (VCL) (i.e. A to B). At B the sample is unloaded and swells travelling along the swelling line BC. On reloading the sample moves along the line CDE. At point D it rejoins the VCL and remains on this line with any further increase in vertical stress. If unloaded again the soil will move along another swelling curve. For example, when unloaded from point E the soil follows the line EF. It is generally assumed that swelling loops, such as BCD and EFG, are parallel.

Soil which is on the VCL is said to be normally consolidated because it has never been subjected to a higher vertical stress. Soil on a swelling loop is defined as overconsolidated, with an overconsolidation ratio (*OCR*) defined as $\sigma_v'_{max}/\sigma_v'$, where $\sigma_v'_{max}$ and σ_v' are the maximum vertical effective stress the sample has ever experienced and the current vertical effective stress, respectively. For an increment of vertical stress normally consolidated soil suffers a much larger change in void ratio than an overconsolidated soil. This implies that overconsolidated soils are much stiffer than normally consolidated soils. Overconsolidated soils subjected to reloading experience a rapid reduction in stiffness as their stress state approaches the VCL.

To use results like those shown in Figure 1 for design purposes simplifications are often introduced. For example, it is often assumed that the VCL is a straight line in e-$\log_{10}\sigma_v'$ space, with a gradient C_c, and that the swelling loop can be replaced with a single line of gradient C_s. However, such an approach is not universally accepted. For example, some geotechnical engineers advocate plotting the results in $\log_{10}e$-$\log_{10}\sigma_v'$ space before making the idealisations for the VCL and swelling loops, while others prefer to plot results in terms of mean effective stress instead of vertical effective stress and/or to use natural logarithms.

When considering the behaviour of a deposit of sedimentary clay, it is recognised that the clay begins its existence in the form of a slurry and that its current state results from a combination of consolidation and swelling stages. It may therefore be considered that all parts of the deposit have a unique starting point, namely, the clay slurry. However, such an assumption is not valid for sands, as sands can be deposited at different rates, resulting in a range of initial densities which influence subsequent behaviour.

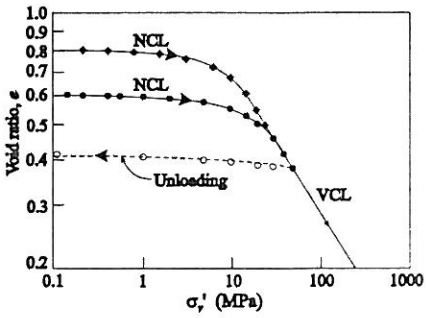

Figure 2: One-dimensional behaviour of Ticino sand (Pestana, 1994)

Figure 2 shows the compression characteristics of two samples of Ticino sand (Pestana, 1994): one initially in a dense state with $e_o = 0.6$, the other in a loose state with $e_o = 0.8$. When the two samples are compressed one-dimensionally, they follow normal compression lines (NCLs) which, at high values of effective stress, approach a unique virgin compression line (VCL). As the samples have different initial void ratios, the NCLs are not coincident. The VCL is approached when the sand particles start to crush. The magnitude of the vertical stress at which this occurs is dependent on the strength of the soil particles (Coop, 1990). For example, for the loose Ticino sand, shown in Figure 2, the VCL is reached only when the vertical effective stress exceeds 10 MPa. For the dense sample an even higher vertical stress is required, due to the greater number of contact points compared to the loose sample. Consequently, the stress levels and behaviour associated with most geotechnical structures usually relate to the early parts of the normal compression curves (NCLs). Unloading/reloading results in hysteresis loops as discussed above for clay, and, although not shown in Figure 2, it is commonly observed that unload/reload loops are parallel when the data is plotted in e-$\log_{10}\sigma_v'$ space.

2.2 Behaviour when sheared

Typical results from a series of triaxial tests performed on K_o consolidated samples of clay from Pentre in Shropshire are shown in Figure 3 (Connolly (2002)). All samples were K_o (i.e. zero radial strain) normally consolidated from A to B, see Figure 3. The samples were then K_o unloaded to a particular value of overconsolidation ratio, with each sample having a different *OCR*. At this point all drainage valves were closed and the samples were sheared undrained to failure, by either increasing or decreasing the axial stress. The resulting effective stress paths are shown in Figure 3. Several important facets of soil behaviour are evident in this plot. Firstly, the effective stress paths

for samples with an $OCR<3$ bend to the left, having a smaller mean effective stress at the end of the test than they had at the beginning. This implies that, when sheared, the samples tried to contract, however, as undrained conditions were enforced this resulted in the generation of compressive (positive) pore water pressures. In contrast, the stress paths for the heavily overconsolidated samples ($OCR \geq 3$) bend to the right. This implies dilatant behaviour and the generation of tensile (negative) pore water pressures.

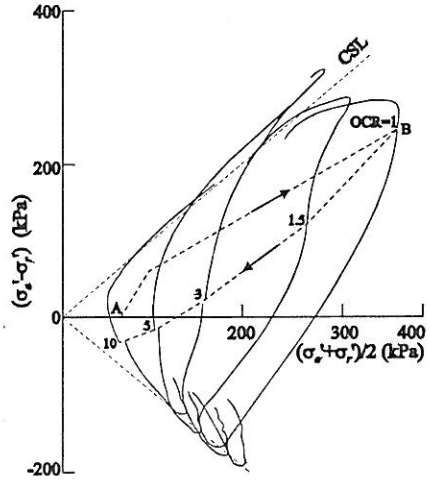

Figure 3: Effective triaxial stress paths for laminated Pentre clay (Connolly, 1999)

The stress states of all samples at failure tend to plot on a straight line which passes through the origin. This line is often referred to as the critical state line and is defined by an angle of shearing resistance, φ_{cs}'. The relevant φ_{cs}' angles for the stress paths shown in Figure 3 are 32° and 28° for compression and extension respectively. Although not evident in Figure 3, sometimes for heavily overconsolidated clay the stress paths pass above the critical state line before they reach failure. This implies a peak effective strength, in terms of a cohesion, c', and an angle of shearing resistance, φ', greater than that at ultimate failure.

For lightly overconsolidated samples the deviator stress ($=(\sigma_a'-\sigma_r')$) reaches a peak value and then reduces as ultimate failure is approached. This implies that the undrained strength, S_u, which is defined as half the maximum deviator stress, occurs before the full angle of shearing resistance has been mobilised. In contrast, for the heavily overconsolidated samples the deviator stress obtains its highest value at ultimate failure.

The variation of secant Young's modulus E_u ($=(\sigma_a-\sigma_{ao})/(\varepsilon_a-\varepsilon_{ao})$, (where σ_{ao} and ε_{ao} are the axial total stress and the axial strain just prior to undrained shearing respectively) with change in axial strain, $\varepsilon_a-\varepsilon_{ao}$, are shown in Figures 4a and 4b, for the compression and extension tests respectively. These plots clearly show that the soil becomes progressively less stiff as it is sheared. This occurs for all samples, but is particularly marked for the lightly overconsolidated samples where the stiffness drops by more than an order of magnitude.

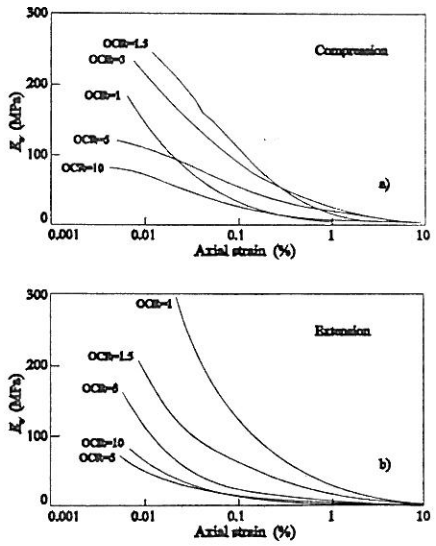

Figure 4: Undrained Young's moduli for Pentre clay (Connolly, 1999)

It is also evident from Figure 4 that the stiffness magnitude depends on OCR. However, it should be noted that both OCR and the mean effective stress, p' ($=(\sigma_1'+\sigma_2'+\sigma_3')/3$), vary for each test. It is therefore not possible to identify the influence of each of these parameters from the data presented. The effect on stiffness of stress level alone is shown in Figure 5 (Soga *et al.* (1995)), where the results from four torsional tests on isotropically normally consolidated kaolin are presented. The tests differ only in that the magnitude of the consolidation stress changes. The results indicate the typical decay of stiffness with strain as shown in Figures 4a and 4b, but more importantly they indicate a nonlinear relationship between stiffness and mean effective stress, p'.

From the above observations it is clear that the overconsolidation ratio and the magnitude of the mean effective stress have a large influence on soil behaviour.

2.3 Effect of stress path direction

The direction of the stress path also affects the stiffness characteristics of the soil. This has been investigated by Smith (1992) who performed a set of triaxial probing tests on Bothkennar clay, see Figure 6. All samples were first consolidated along path ABC and then swelled to D. K_o conditions were applied over

portions BC and CD of this stress path. At point D the samples were allowed to age before being sheared drained along a variety of stress path directions. The variation of stiffness with strain for the probing stages of these tests is shown in Figures 7 and 8. In Figure 7 the equivalent tangent bulk modulus, K_{tan}' ($=\Delta p'/\Delta\varepsilon_v$), normalised by the mean effective stress, p', is plotted against accumulated volumetric strain from the start of the probing stage, ε_v. The equivalent tangent shear modulus, G_{tan} ($=\Delta(\sigma_a'-\sigma_r')/3\Delta\varepsilon_s$), normalised by p' is plotted against accumulated triaxial deviatoric strain from the start of the probing stage, ε_s ($=2/3(\varepsilon_a-\varepsilon_r)$), in Figure 8. Both of these plots indicate that the soil stiffness decreases as the sample is strained and in this respect agree with the data given in Figure 4 for Pentre clay. However, they also show that the magnitude of the stiffness and the manner in which it decays with strain depend on the direction of the probing stress path. Also shown on Figure 8 is the value of the shear modulus, $G_{seismic}$, obtained from seismic tests performed at Bothkennar.

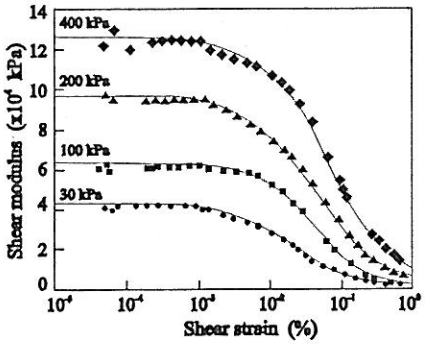

Figure 5: Dependence of kaolin stiffness on stress level (Soga et al. (1995)

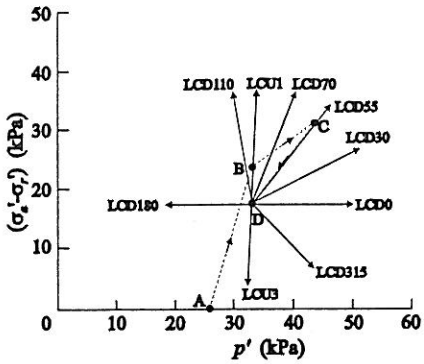

Figure 6: Probing stress paths for Bothkennar clay (Smith, 1992)

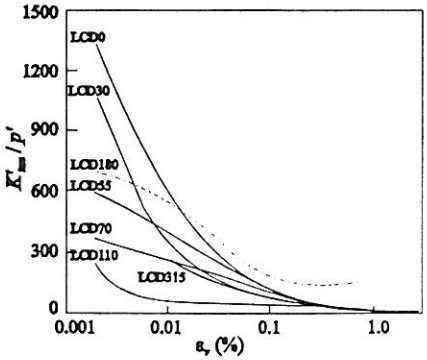

Figure 7: Bulk stiffness for Bothkennar clay (Smith, 1992)

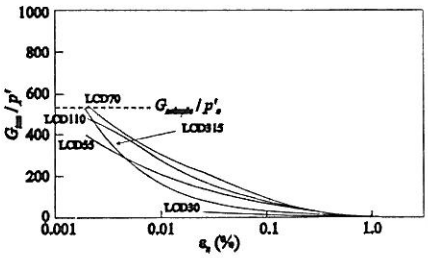

Figure 8: Shear stiffness for Bothkennar clay (Smith, 1992)

2.4 Effect of the magnitude of the intermediate principal stress

As noted above, the drained strength parameters of clay differ depending on whether the clay is subjected to triaxial compression or extension. Similar behaviour is observed for other soils. In compression tests the intermediate principal stress, σ_2, is equal to the minor principal stress, σ_3, and the major principal stress, σ_1, is vertical (i.e. $\alpha = 0°$). In contrast, in extension tests the intermediate principal stress, σ_2, equals the major principal stress, σ_1, and the latter stress now acts horizontally (i.e. $\alpha = 90°$). Consequently, the strength difference could result from the magnitude of the intermediate principal stress, σ_2, or the orientation, α, of σ_1, or a combination of both. In order to investigate the influence of the magnitude of the intermediate principal stress, σ_2, results from isotropically compressed drained true triaxial tests on dense Cumbria sand are considered in Figure 9 (Ochiai & Lade, 1983). In these tests the orientation of the sample was maintained the same and the major principal stress always acted in the vertical direction (i.e. $\alpha = 0°$). The samples were all sheared in a similar manner, with the exception that the relative magnitude of the intermediate principal stress differed from test to test. In Figure 9 the relative magnitude of the

intermediate stress is expressed by the value of b ($=(\sigma_2-\sigma_3)/(\sigma_1-\sigma_3)$) and is plotted against the effective angle of shearing resistance, φ'. It can be seen that there is an increase of up to 9° in φ' as the intermediate principal stress increases from being equal to σ_3 ($b=0$) towards σ_1 ($b=1$).

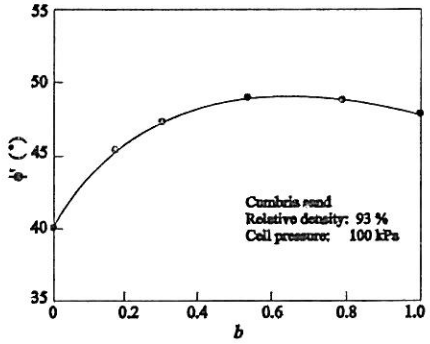

Figure 9: Effect of b on φ' for sand (Ochiai & Lade, 1983)

2.5 Anisotropy

For convenience, laboratory test data are usually interpreted assuming that the soil behaves in an isotropic manner. This is evident in the data presented above, where equivalent isotropic measures of stiffness have been used. In general, soil is unlikely to be completely isotropic, because of the way in which it was originally deposited. In fact, it is only likely to be isotropic in the plane normal to its direction of deposition. Such a material is usually called 'cross anisotropic' or 'transversely isotropic'. In such a material both strength and stiffness depend on both the magnitude and orientation of the applied stresses. However, it is not easy to investigate the anisotropic behaviour of soils in conventional laboratory triaxial and shear box tests. This is one of the reasons why anisotropic effects have been neglected in the past. However, in recent years special testing devices (e.g. directional shear cell and hollow cylinder apparatus) have been developed to investigate anisotropic effects and, consequently, limited data exist.

Data on the undrained shear strength of K_o consolidated reconstituted Boston Blue clay are presented in Figure 10. These data come from a series of tests performed in a directional shear cell by Seah, 1990, in which similar samples were sheared with different orientations of the major principal stress to the direction of deposition, α (see insert in Figure 10). In Figure 10 the undrained shear strength, S_u, normalised by the vertical consolidation stress, σ_p' (i.e. vertical stress after K_o consolidation/swelling), is plotted against α, for normally consolidated clay and clay with an OCR=4. It can be seen that the undrained strength drops significantly, by up to 50%, as α increases, indicating a strong anisotropic effect. If the clay was isotropic, the undrained strength would be unaffected by the value of α.

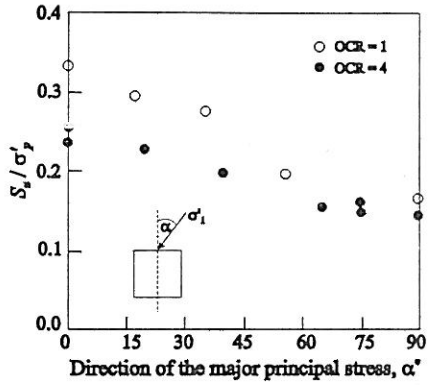

Figure 10: Undrained strength anisotropy of Boston Blue clay (Seah, 1990)

Results from a series of hollow cylinder tests performed on K_o normally compressed Ham River sand are presented in Figure 11, in the form of the peak angle of shearing resistance, φ_p', against α (Hight, 1998). All the tests had b = 0.3 and were similar except for the value of α. The results indicate a marked variation of φ_p' with α. The effect of changing α is large, indicating a high degree of anisotropy in the sand, much larger than that observed for clay soils.

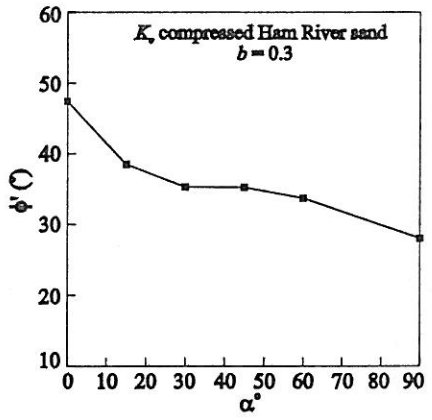

Figure 11: Effect of α on φ' for sand (Hight, 1998)

Soils also exhibit anisotropic stiffness behaviour. This can be seen in Figure 12 which shows results from Kohata *et al.*, 1997, who tested prismatic samples of a range of sands and gravels. For each soil type a series of samples were normally compressed with different ratios of the vertical and horizontal effective stress, σ_v'/σ_h'. The samples were then subjected to small cycles of both vertical and horizontal loading

from which small strain values of E_v' and E_h' could be calculated. The results from three sands, Toyoura, SLB and Ticino, are shown in Figure 12 where the ratio E_v'/E_h' is plotted against the ratio σ_v'/σ_h'. If the samples were isotropic then $E_v'/E_h'=1$, however, the greater the departure from this value the larger the anisotropy.

The results show that for all three sands the degree of anisotropy changes with σ_v'/σ_h'. The results also show that the amount of anisotropy is much larger for SLB sand than for both Toyoura and Ticino sand.

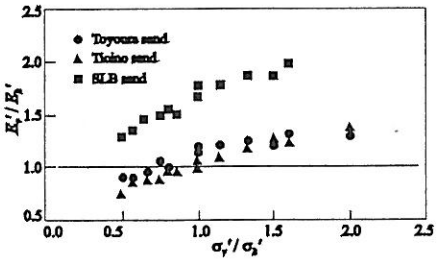

Figure 12: Stiffness anisotropy of sands (Kohata *et al.*, 1997)

3 LINEAR ELASTIC PLASTIC MODELS

In circumstances where there are no sensitive structures or installations close by, it may be possible to use very simple models to analyse deep excavations. For example Fernie *et al.*, 1996 described the design and performance of the Eastbourne Wastewater Treatment Scheme at Langley Point, a 14m deep box very close to the English Channel. Figure 13 shows the soil profile and a section through the structure containing the Works.

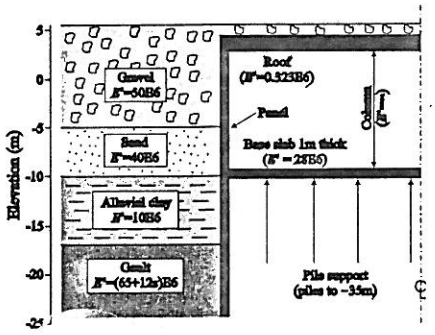

Figure 13: Cross-section for the Wastewater Works at Langley Point

To form the excavation, ground within the box was de-watered, which was only turned off after the base slab had been constructed, allowing pore water pressures under the slab to return to the levels that existed before construction started. Piles linked to the base slab restrained floatation in the long term.

Although movements remote from the excavation were not an issue, movements of the walls and structural forces in the walls and base slab were. Finite element analyses were therefore carried out. From the site investigation it was possible to determine the soil stratigraphy and estimate values of soil strength. However, it was only possible to obtain limited information on soil stiffness. Consequently, a very simple linear elastic perfectly plastic (Mohr-Coulomb) constitutive model was employed to represent the soil. The structural members were assumed to be linear elastic.

Figure 14 compares predictions of wall displacement (made before construction) with the field observations for the situation when construction had been completed. It can be seen that the agreement between prediction and observation is good. Because of the restraint afforded by the piles beneath the base slab, the behaviour of the structure depended to a large extent on the changes in water pressure acting on it. There was therefore relatively little soil structure interaction. The comparatively simple soil model performed adequately and it is unlikely that the use of a more sophisticated model would have given predictions in much better agreement with the observations.

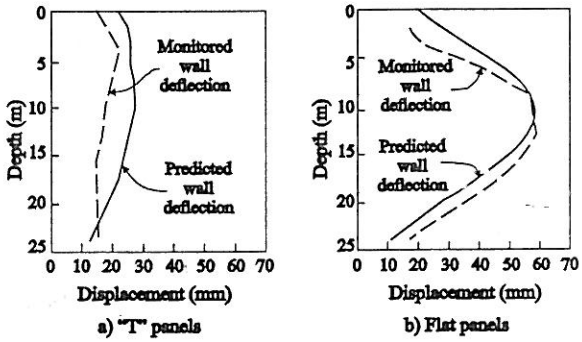

Figure 14: Predicted and observed wall displacements for two types of panels

It is worth noting that the predictions of the soil movements remote from the box walls were not realistic. Another situation where the use of such simple models does not provide accurate predictions is the analysis of surface subsidence due to tunnelling. Figure 15 shows predictions and field measurements from the recently constructed Jubilee Line extension in London. The results presented are for the construction of the first running tunnel beneath St. James's Park (Nyren, 1998). Being a park, the ground movements were not influenced by surface structures. Soil conditions consist of London Clay, in which the tunnel is constructed, overlain by Thames Gravel and Made

Ground. Soil parameters were obtained from a comprehensive site investigation.

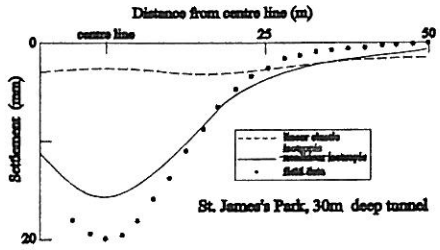

Figure 15: Effect of a pre-yield model on predicted settlement profile

Results based on a simple linear elastic plastic model of the same type as used for the excavation problem discussed above are shown by the dashed line. Clearly they are not in agreement with the field data. The predicted settlement profile is of the wrong shape, being too shallow and too wide when compared to the field data. Such results are typical of predictions of tunnel induced movements in stiff overconsolidated clays based on simple linear elastic perfectly plastic constitutive soil models (Potts & Zdravkovic, 2001).

4 SMALL STRAIN STIFFNESS

The reason why the simple linear elastic perfectly plastic model was unable to accurately predict the soil movements remote form the wall in the excavation problem, and failed totally to predict realistic subsidence troughs above tunnels in stiff clay, is that soil behaviour is nonlinear even at small strain levels. For example, Figure 16 shows the secant shear modulus (normalised by mean effective stress p') decay with shear strain observed in triaxial tests on London Clay. It is clear that even under small strain perturbations the soil behaviour is nonlinear.

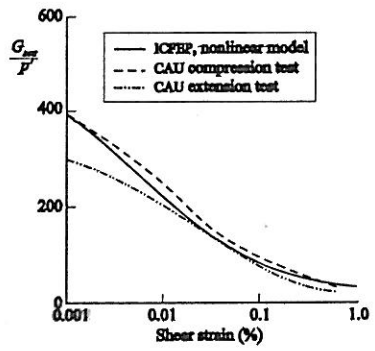

Figure 16: Small strain curves from triaxial tests

As the site investigation data for the Jubilee line extension included laboratory triaxial tests equipped with devices to accurately measure small strains, it is possible to include this behaviour into a constitutive model. The simplest way, but not necessarily the best way, is to account for the small strain behaviour by replacing the linear elastic parameters in the simple model by a nonlinear elastic model (see Addenbrooke *et al.*, 1997 and Potts & Zdravkovic, 2001).

Figure 16 shows that such a model is capable of capturing the behaviour observed in the laboratory. The result of using the model to predict the subsidence trough above the Jubilee Line extension tunnel at St. James's Park is shown in Figure 15. Clearly, the predictions are in much better agreement with the observations than those based on the simpler linear elastic plastic model.

Adjacent to St. James's Park, and across the road from where the greenfield measurements shown in Figure 16 were obtained, is the Treasury building, see Figure 17. As can be seen, the running tunnels of the Jubilee Line extension pass obliquely under the corner of the building. Finite element analyses, using the same nonlinear elastic plastic constitutive model, were performed to model the tunnel induced response of the building. Again these could be compared with field observations. Only a summarised description of the analyses and the results are included here, further details are given in Standing *et al.*, 1998.

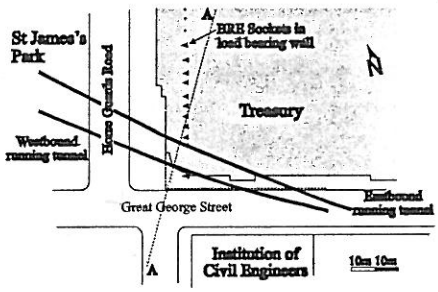

Figure 17: Plan of Treasury site

The Treasury is a massive stone-clad brick-masonry structure, approximately 210m long and 100m wide, with four storeys above ground and two basement levels. The foundations consist of strips and pads connected by an unreinforced concrete slab founded in the Terrace Gravels which overlie London Clay. As part of the Jubilee Line extension project, two running tunnels were excavated under one corner of the building (shown in plan in Figure 17). The westbound tunnel was the first to be excavated. Following this there was a rest period before compensation grouting and excavation of the eastbound tunnel. Compensation grouting was implemented after driving the westbound

tunnel and during construction of the eastbound tunnel. The level of the tubes-a-manchette (TAMs) used for this work was approximately 16m below ground level, see Figure 18, extending beneath the basement between the tunnels and the foundation slab.

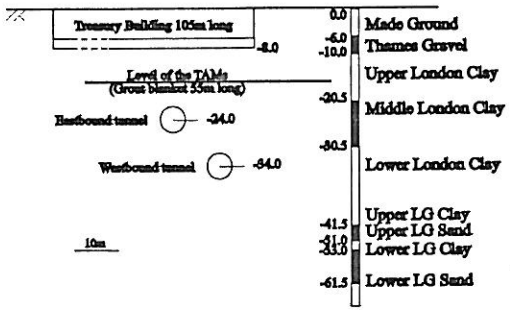

Figure 18: Cross-section through Treasury site

Figure 19 shows settlement troughs after excavation and construction of the westbound (WB) tunnel (i.e. the first tunnel to be constructed). Field measurements at ground surface from St. James's Park (greenfield) and at foundation level of the Treasury are presented. Comparison of observations from these two sites indicates the influence of the building. It reduces the maximum settlement, but increases the width of the settlement trough. The maximum settlement beneath the Treasury is beneath its corner, slightly offset from the tunnel centre-line. Also shown is the finite element prediction. The agreement between the prediction and field observations is excellent.

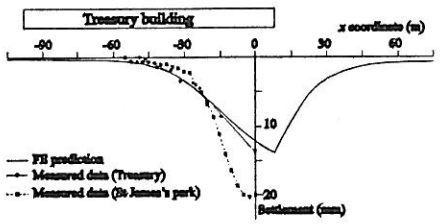

Figure 19: Settlement trough after WB tunnel construction

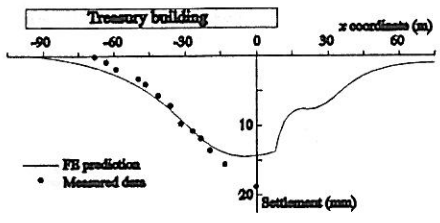

Figure 20: Settlement trough 18 weeks after EB tunnel construction

Figure 20 presents settlement troughs at foundation level for the Treasury, 18 weeks after construction of the eastbound tunnel (EB). Both observation and finite element predictions are presented. The agreement between predictions and observation is again excellent.

Another example which shows the merits of accounting for small strain soil behaviour concerns the installation of an oil platform. The installation of the Hutton tension leg platform (TLP) in the northern North Sea represented an important development in offshore engineering. The use of large driven piles as tension anchors was novel and a number of special studies were undertaken to help design the foundations and validate their performance in service (Jardine & Potts, 1988 and Jardine *et al.*, 1988).

One area of concern was the vertical movement of the anchor piles. As shown in Figure 21, the TLP foundations consisted of four clusters of eight piles, one cluster at each corner of the platform. The piles were 1.83m in diameter and 60m long. To monitor movements of the pile clusters 'settlement gauges' were installed on the sea bed. These gauges were of the manometer type and the position of one such gauge is indicated on Figure 21. As the gauges were installed to provide early warning of any likely problems with the anchor piles, it was necessary to estimate the movements that were likely to occur. Comparison of measured movements with these predictions would enable the performance of the piles to be assessed.

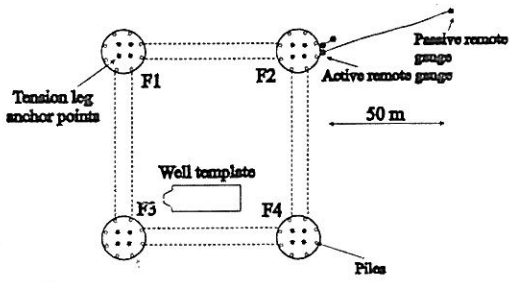

Figure 21: Layout of Hutton TLP platform

In conventional pile group design movements are calculated assuming the soil to be essentially linear elastic and predictions are usually conservative if they are greater in magnitude than those observed in the field. However, for the Hutton TLP situation conservative estimates of movement would need to be smaller in magnitude than those observed (i.e. it is necessary to underpredict the displacement at which the piles pull out). Selecting soil stiffness values based on experience with conventional pile design was therefore not appropriate

To obtain a more accurate estimate of soil stiffness, laboratory triaxial tests were performed in which the samples were fitted with local strain instrumentation. These provided accurate data on soil stiffness and in particular how it varied with strain level. Such data

was then used to establish theoretical nonlinear elastic relationships for how the elastic shear and bulk moduli varied with both stress and strain level. These were then incorporated into a form of the modified Cam Clay model and used in a finite element analysis to predict the behaviour of the Hutton TLP foundations. It should be noted that a simple plasticity model, such as Mohr-Coulomb, was not appropriate, as the clay soils at Hutton had relatively low overconsolidation ratios.

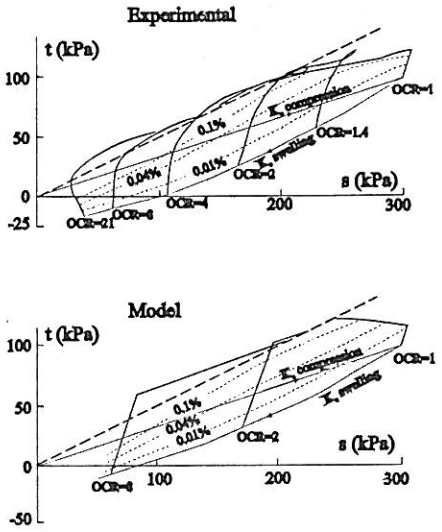

Figure 22: Experimental and simulated triaxial stress paths

A comparison of results from some of the triaxial tests with predictions from the constitutive model is presented in Figure 22. Clearly the model is capable of capturing the main facets of the observed soil behaviour. During platform installation the tethers connecting the foundations to the buoyant deck were pre-tensioned. For each pile cluster there were four tethers and these were tensioned to give an upward force of approximately 3000 tonnes. During this process the movements of the anchor piles were observed. These movements are plotted against tether load for pile cluster F2 in Figure 23. Also shown on this figure are predictions from the finite element analysis (made before the event) and from conventional pile group analysis based on isotropic elastic soil behaviour. Clearly, the latter predictions are not in agreement with the observations, predicting too large movements. In this respect they are not conservative. In comparison, the predictions from the finite element analyses, which take account of the small strain soil behaviour, are in excellent agreement with the observations. As noted by Jardine & Potts, 1988 the finite element analysis was able to accurately capture many other aspects of the observations. This example clearly indicates the importance of accounting for small strain soil behaviour.

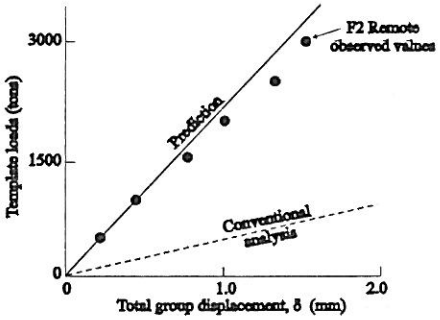

Figure 23: Observed and predicted displacement of Hutton TLP piles

5 CHOICE OF SOIL MODEL

In the previous section it has been shown that it is often necessary to account for the small strain behaviour of soil in any geotechnical analysis. In the examples presented this small strain behaviour has been accounted for using a nonlinear elastic formulation within a conventional plasticity model (i.e. either Mohr-Coulomb or modified Cam Clay). In this section the alternative of modelling the small strain behaviour in terms of an elasto-plastic formulation will be investigated. Again, results from a case history will be used.

Roadford dam is a 41m high rockfill dam that has recently been constructed in the United Kingdom. It has an upstream asphaltic concrete membrane and a typical cross section of the dam is shown in Figure 24. Details of the design of the dam and of the properties of the rockfill are given by Wilson & Evans, 1990. As indicated on Figure 24, instrumentation was installed in the dam to monitor its behaviour.

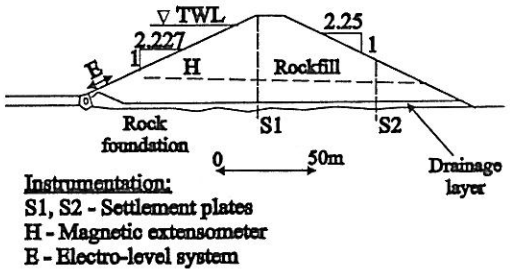

Figure 24: Cross-section through Roadford dam

Finite element analysis of the dam was performed using two different constitutive models (Potts & Zdravkovic, 2001). One of these models was a nonlinear elastic perfectly plastic (Mohr-Coulomb) model. The other was a complex work

hardening/softening elasto-plastic model of the Lade type, having a double yield surface. In both cases the model parameters were determined from standard oedometer and triaxial laboratory tests. A comparison of the predictions from the constitutive models with the laboratory data is shown in Figures 25 and 26. While both models are able to accurately reproduce the oedometer behaviour and the shear stress - strain triaxial data, the nonlinear elastic-perfectly plastic model has difficulty in reproducing the volumetric strain behaviour observed in the triaxial tests. Adjustments to the model parameters enabled a slightly better fit to be obtained, but this was at the expense of a less good fit to the shear stress - strain and oedometer data.

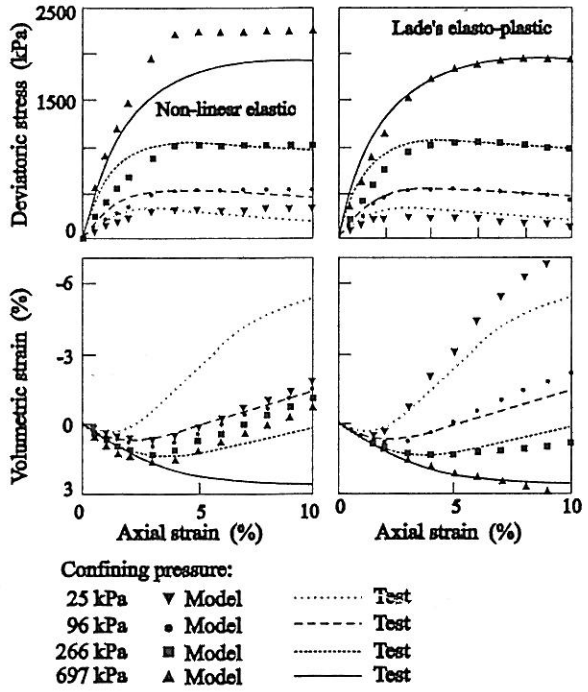

Figure 25: Simulation of triaxial tests

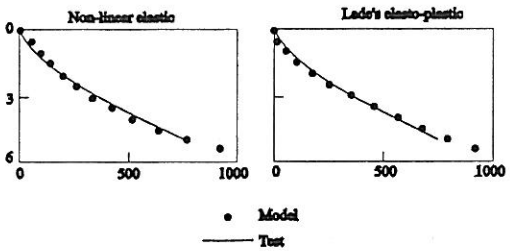

Figure 26: Simulation of oedometer tests

A comparison between the finite element predictions and the observations from the settlement gauges S1 and S2, see Figure 24, during construction of the dam are shown in Figure 27. Analyses using both soil models give reasonable agreement with the observations. It should be noted that even better agreement could be reached if account was taken of the fact that the top part of the dam was constructed at a higher relative density then assumed at the design stage. However, such agreement between the two analyses is not so good for horizontal movements, as can be seen in Figure 28 which compares predictions with observations from the horizontal gauge, H (see Figure 24). While the analyses using the complex Lade model give horizontal movements in agreement with the observations, those from the analysis using the simpler model are inaccurate. The reason for the success of the complex model and the failure of the simpler model to predict horizontal displacements is that in the former both elastic and plastic components of strain are mobilised, whereas in the latter only elastic strains are developed during construction. It appears that while such a detail is not important for the prediction of vertical displacements, it is for accurate prediction of horizontal displacements.

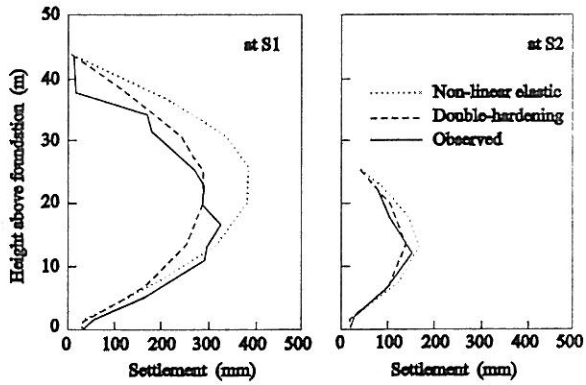

Figure 27: Comparison of predicted and observed settlements

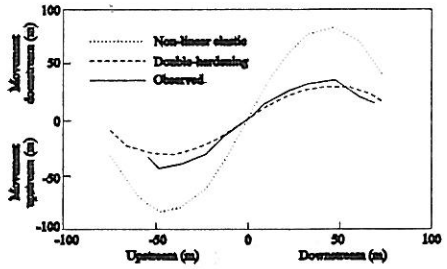

Figure 28: Comparison of predicted and observed horizontal displacements

It should be noted that for this dam accurate prediction of horizontal movements was important, especially during impounding, as it was the behaviour of the upstream membrane and its connection with the upstream toe inspection gallery that was of concern. The observation that analysis based on nonlinear elastic behaviour pre-yield have difficulties in predicting the measured horizontal movements was

also reported by Potts *et al.*, 1990 when analysing the failure of Carsington dam.

6 MODEL FORMULATION IN THE DEVIATORIC PLANE

As noted above, when discussing the behaviour of real soil, the magnitude of the intermediate stress can have a significant effect on soil behaviour, especially its strength. To illustrate the importance of this facet of soil behaviour the effect of the shape of the yield and plastic potential surfaces on soil strength will now be considered. This is demonstrated by using the modified Cam clay model to show that what seems like sensible input parameters can result in unrealistic predictions. Experience indicates that this is a very common pitfall that many users unknowingly fall into, with the result that their analyses predict erroneous collapse loads which are usually unconservative.

Modified Cam clay (Roscoe & Burland, 1968), like the original Cam clay model, was developed for triaxial loading conditions. The model is essentially based on the following assumptions:

- Isotropic drained compression of a clay sample generates a virgin consolidation line (VCL) of inclination λ in v-lnp' space (see Figure 29). Similarly, isotropic drained swelling of clay follows a swelling line of inclination κ in v-lnp' space. Volume change along the VCL is mainly irreversible or elasto-plastic, while volume change along a swelling line is reversible or elastic.

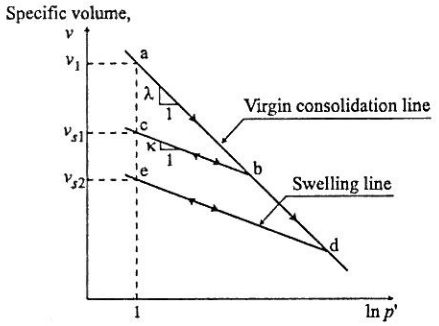

Figure 29: Behaviour under isotropic compression

- The behaviour under increasing triaxial shear stress, $q=\sigma_v'-\sigma_h'=\sqrt{3}J$, (where $J=[(\sigma_1'-\sigma_2')^2+(\sigma_2'-\sigma_3')^2+(\sigma_1'-\sigma_3')^2]^{0.5}*(1/\sqrt{6})$) is assumed to be elastic until a yield value of q is reached, which can be obtained from the yield function $F(\{\sigma'\},\{k\}) = 0$. As noted above, behaviour is elastic along swelling lines and therefore the yield function plots above each swelling line as shown in Figure 30. For modified Cam clay the yield surface is assumed to take the form:

$$F(\{\sigma'\},\{k\}) = \left(\frac{J}{p'M_J}\right)^2 - \left(\frac{p_o'}{p'} - 1\right) = 0 \qquad (1)$$

where p' is the mean effective stress, J is the deviatoric stress, M_J is another clay parameter, and p_o' is the value of p' at the intersection of the current swelling line with the virgin consolidation line, see Figure 30. The parameter p_o' essentially controls the size of the yield surface and has a particular value for each swelling line. As there is a yield surface for each swelling line, the yield function, given by Equation (1) defines a surface in v-J-p' space, called the *Stable State Boundary Surface.*

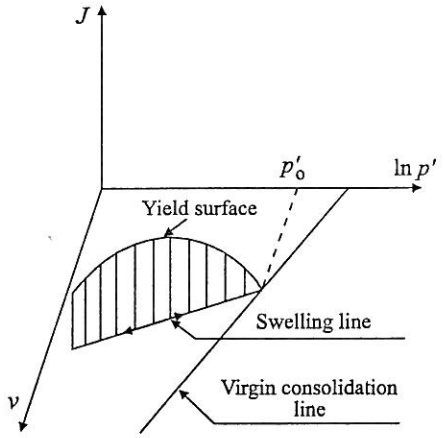

Figure 30: Yield surface

- Hardening/softening is isotropic and is controlled by the parameter p_o' which is related to the plastic volumetric strain, ε_v^p, by:

$$\frac{dp_o'}{p_o'} = d\varepsilon_v^p \frac{v}{\lambda-\kappa} \qquad (2)$$

Equation (2) therefore provides the hardening rule.

- When the soil is plastic (i.e. on the Stable State Boundary Surface), the plastic strain increment vector is taken normal to the yield curve. Consequently, the model is associated, with the plastic potential $P(\{\sigma'\},\{m\})$ being given by Equation (1).
- As noted above, behaviour along a swelling line is elastic. This means that the elastic volumetric strain, ε_v^e, can be determined from:

$$d\varepsilon_v^e = \frac{dv}{v} = \frac{\kappa}{v}\frac{dp'}{p'} \qquad (3)$$

This gives the elastic bulk modulus, K, as:

$$K = \frac{dp'}{d\varepsilon_v^e} = \frac{vp'}{\kappa} \quad (4)$$

In the original formulation, no elastic shear strains are considered. To avoid numerical problems and to achieve a better modelling inside the state boundary surface, elastic shear strains are usually computed from an elastic shear modulus, G, which is an additional model parameter.

In the above form, the modified Cam clay model requires five material parameters: v_1 , λ, κ, M_J and G. Sometimes an elastic Poisson's ratio, μ, is specified instead of G.

The original critical state formulation is based, almost exclusively, on laboratory results from conventional triaxial tests. The portions of stress space in which these tests operate are severely restricted as the intermediate principal stress must be equal to either the major or the minor principal stress. Because of this, the basic formulation is developed in terms of q ($=\sigma_1'-\sigma_3'$) and p'. For numerical analysis, the models have to be generalised to full stress space by making some assumption on the shape of the yield surface and plastic potential in the deviatoric plane. The first generalisation is achieved by effectively replacing q by J. This substitution is made in Equation (1). In general stress space this is equivalent to assuming that the yield and plastic potential surfaces (and hence the failure surface) are circles in the deviatoric plane, see Figure 31. However, it is well known that a circle does not represent well the failure conditions for soils, where a Mohr-Coulomb type failure criterion is more appropriate. Roscoe and Burland, 1968 suggest that circular (in the deviatoric plane) yield surfaces should be used combined with a Mohr-Coulomb failure criterion. This implies, however, that critical state conditions can only be reached under triaxial compression conditions ($\sigma_2'=\sigma_3'$).

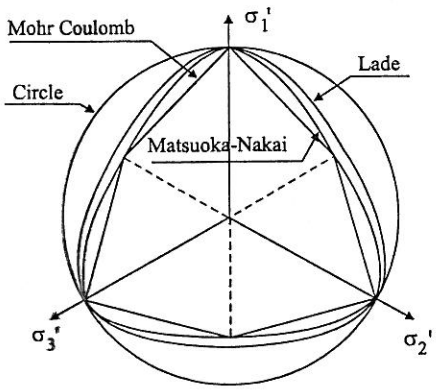

Figure 31: Failure surfaces in the deviatoric plane

In order to obtain a Mohr-Coulomb hexagon for the yield surface in the deviatoric plane, M_J in Equation (1) must be replaced by $g(\theta)$:

$$g(\theta) = \frac{\sin\varphi_{cs}'}{\cos\theta + \frac{\sin\theta\sin\varphi_{cs}'}{\sqrt{3}}} \quad (5)$$

where θ is the Lode's angle ($=\tan^{-1}[(2(\sigma_2'-\sigma_3')/(\sigma_1'-\sigma_3')-1)/\sqrt{3}]$), φ_{cs}' is the critical state angle of shearing resistance which replaces M_J as an input parameter. This expression gives the hexagon shown in Figure 31. Equation (1) then becomes:

$$F(\{\sigma'\},\{k\}) = \left(\frac{J}{p'g(\theta)}\right)^2 - \left(\frac{p_o'}{p'} - 1\right) = 0 \quad (6)$$

Critical state conditions then occur with a constant φ_{cs}'.

Other failure surfaces have been suggested which are continuous and agree better with experimental results in the deviatoric plane. Matsuoka and Nakai's (1974) and Lade's (Lade & Duncan, 1975) are the best known, see Figure 31. These surfaces can also be expressed using an appropriate function for $g(\theta)$, (Potts & Zdravkovic, 1999).

The importance of the model formulation in the deviatoric plane is highlighted by Potts & Zdravkovic, 1999. They demonstrate that the adoption of a plastic potential shape, $g_{pp}(\theta)$, in the deviatoric plane and a dilation angle, v, determines the value of the Lode's angle at failure, θ_f, in problems involving plane strain deformation. They show that some of the plastic potential expressions proposed in the literature do not guarantee realistic values of θ_f. They indicate that it is often necessary to have different shapes of the yield and plastic potential surfaces in the deviatoric plane.

As noted above, the shape of the plastic potential in the deviatoric plane can affect the Lode's angle θ at failure in plane strain analyses. This implies that it will affect the value of the soil strength that can be mobilised. In many commercial software packages, the user has little control over the shape of the plastic potential and it is therefore important that its implications are understood.

Many software packages assume that both the yield and plastic potential surfaces plot as circles in the deviatoric plane. This is defined by specifying a constant value of the parameter M_J. Such an assumption implies that the angle of shearing resistance, φ', varies with the Lode's angle, θ. By equating M_J to the expression for $g(\theta)$ given by Equation (5) and re-arranging, gives the following expression for φ' in terms of M_J and θ:

$$\varphi' = \sin^{-1}\left(\frac{M_J \cos\theta}{1 - \frac{M_J \sin\theta}{\sqrt{3}}}\right) \quad (7)$$

From this equation it is possible to express M_J in terms of the angle of shearing resistance, φ'_{TC}, in triaxial compression ($\theta = -30°$), see Equation (8):

$$M_J(\varphi'_{TC}) = \frac{2\sqrt{3}\sin\varphi'_{TC}}{3 - \varphi'_{TC}} \quad (8)$$

In Figure 32 the variation of φ' with θ, given by Equation (7), for three values of M_J is plotted. The values of M_J have been determined from Equation (8) using φ'_{TC}=20°, 25° and 30°. If the plastic potential is circular in the deviatoric plane, it can be shown, (Potts & Zdravkovic, 1999), that plane strain failure occurs when the Lode's angle θ=0°. Inspection of Figure 32 indicates that for all values of M_J there is a large change in φ' with θ. For example if M_J is set to give φ'_{TC}=25°, then under plane strain conditions the mobilised φ' value is φ'_{PS}=34.6°. This difference is considerable and much larger than indicated by careful laboratory testing. The difference between φ'_{TC} and φ'_{PS} becomes greater the larger the value of M_J.

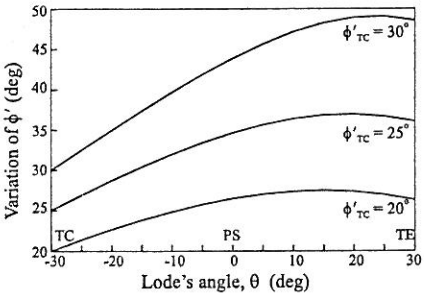

Figure 32: Variation of φ' with θ for constant M_J

To investigate the effect of the shape of the yield and plastic potential surfaces in a boundary value problem, two analyses of a rough rigid strip footing have been performed. The modified Cam clay model was used to represent the soil which had the following material parameters: OCR=6, v_1=2.848, λ=0.161, κ=0.0322 and μ=0.2. In one analysis the yield and plastic potential surfaces were assumed to be circular in the deviatoric plane. A value of M_J = 0.5187 was used for this analysis, which is equivalent to φ'_{TC}=23°. In the second analysis a constant value of φ'=23° was used, giving a Mohr-Coulomb hexagon for the yield surface in the deviatoric plane. However, the plastic potential still gave a circle in the deviatoric plane and therefore plane strain failure occurred at θ=0°, as for the first analysis. In both analysis the initial stress conditions in the soil were based on a saturated bulk unit weight of 18kN/m^3, a ground water table at a depth of 2.5m and a K_o = 1.227. Above the ground water table the soil was assumed to be saturated and able to sustain pore water pressure suctions. Coupled consolidation analyses were performed but the permeability and time steps were chosen such that undrained conditions occurred. Loading of the footing was simulated by imposing increments of vertical displacement.

In summary, the input to both analysis is identical, accept that in the first, the strength parameter M_J is specified, whereas in the second, φ' is input. In both analyses φ'_{TC}=23° and therefore any analyses in triaxial compression would give identical results. However, the strip footing problem is plane strain and therefore differences are expected. The resulting load displacement curves are given in Figure 33. The analysis with a constant M_J gave a collapse load some 58% larger than the analysis with a constant φ'. The implications for practice are clear, if a user is not aware of the plastic potential problem and/or is not fully conversant with the constitutive model implemented in the software being used, he/she could easily base the input on φ'_{TC}=23°. If the model uses a constant M_J formulation, this would then imply a φ'_{PS}=31.2°, which in turn leads to a large error in the prediction of any collapse load.

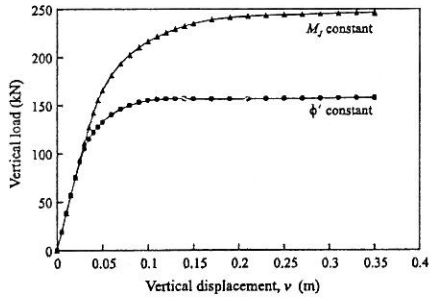

Figure 33: Load-displacement curves for two different approaches

7 ANISOTROPIC SOIL BEHAVIOUR

In all the analyses described above soil behaviour was assumed to be isotropic. This is a common assumption, even though most soils are likely to be anisotropic as a result of the way they were formed (i.e. one dimensional sedimentation). One of the reasons for making such an assumption is that it is difficult to investigate anisotropic behaviour with standard laboratory tests. There are only a few pieces of equipment, such as the hollow cylinder apparatus

and the directional shear device, which allow simultaneous control of both the magnitude of the intermediate principal stress and the direction of the principal stresses. Such control is needed for a systematic investigation of both inherent and induced anisotropy. Recent research using such equipment has clearly shown that many soils are anisotropic in their behaviour.

To indicate the likely effects of soil strength anisotropy, a case history involving the construction of an embankment on soft ground will be considered.

The Champlain Clay covers a large part of a densely populated region of Eastern Canada. Construction of the road infrastructure requires numerous overpasses, containing embankments approximately 5m in height. As the clay is only lightly overconsolidated, it is soft and weak and it is therefore difficult to design and construct embankments to the required height.

For this reason the geotechnical group of Laval University decided in 1972 to undertake a research programme involving the construction of test embankments on soft Champlain deposits. The objective of this project was to investigate the failure conditions of fills built on soft, sensitive foundations and also to study the magnitude and rate of settlement of such structures. Four embankments were constructed on instrumented clay foundations at the Saint-Alban site in the Province of Quebec: the first one, which is the subject of this study, was built until failure occurred; three others were built to a smaller height and with different side slopes in order to study settlement behaviour.

Test embankment A, described by La Rochelle *et al.*, 1974, was the subject of finite element analyses (Zdravkovic *et al.*, 2002), with the objective of investigating the effect of anisotropic soil behaviour on embankment height at failure.

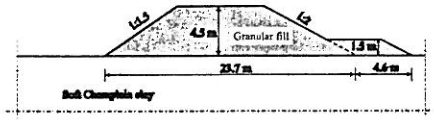

Figure 34: Geometry of test embankment at Saint-Alban

The geometry of this boundary value problem is presented in Figure 34. One side of the embankment has a slope of 2:1 (horizontal to vertical) inclination. The stability of this slope is enhanced by the presence of 1.5 m heigh berm, so that any failure is forced onto the other side of the embankment, where the slope is steeper, with 1.5:1 inclination. The predicted height of the embankment, based on conventional limit equilibrium analysis, was 4.6 m.

The construction sequence was such that the first 0.6m of embankment was lifted in a day, followed by 0.3m per day until a height of 1.5m was reached. After that two 0.3m layers were lifted per day, until failure occurred at an embankment height of 3.9m, which was less than the predicted 4.6m.

A detailed geotechnical investigation was carried out at the Saint-Alban site, with a substantial number of boreholes and both in-situ and laboratory experiments on Champlain Clay samples. Details of the results of these tests are given by Tavenas & Chapeau, 1973 and Sarrailh & Tavenas, 1972.

In general, the soil profile on the site has a weathered clay crust extending down to ~2.0 m below the ground surface, followed by a soft silty marine clay deposit down to ~13.7 m. Beneath this clay layer there is a layer of a dense, fine to medium sand, followed by bedrock. Ground water level is at 0.7 m below the ground surface. The embankment fill is granular.

For the finite element analyses, these foundation soil conditions were modelled using both the MIT-E3 soil model (to simulate anisotropic soil strength) and the modified Cam Clay soil model, MCC (to simulate isotropic soil strength).

The undrained strength variation with depth for different loading conditions, simulated by the MIT-E3 model, is presented in Figure 35. It can be seen from this figure that the predicted direct simple shear strength (DSS) matches, on average, the strength obtained from vane tests. Also, the simulated CIU strengths match closely the experimental CIU strengths. It can therefore be concluded that the observed anisotropic strength has been modelled very well with the MIT-E3 model. Also presented in Figure 35 are the profiles of plane strain compression (PSC) and plane strain extension (PSE) undrained strength.

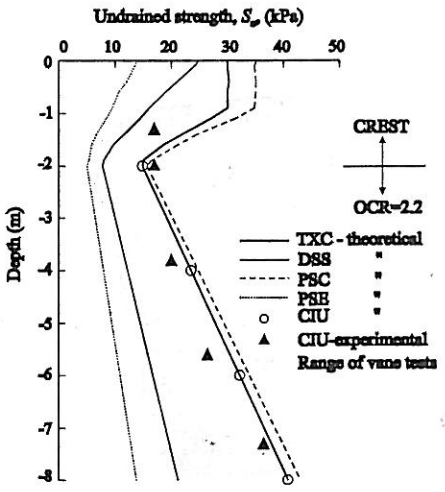

Figure 35: Undrained strength profiles at Saint-Alban

For the isotropic analyses, the undrained strength in triaxial compression was adopted and the modified Cam Clay model was used to simulate the triaxial compression strength profile (TXC), as predicted by the MIT-E3 model in Figure 35.

The same construction sequence and rate were simulated as those implemented on site, such that failure occurred under undrained conditions. Figure 36 shows the development of horizontal displacement, u, of the embankment toe with the embankment height. This horizontal displacement is normalised by the maximum horizontal displacement, u_{max}, predicted just before the slope failed.

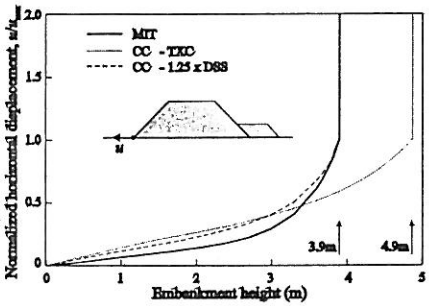

Figure 36: Failure of Saint-Alban embankment - original geometry

The analysis performed using the MIT-E3 soil model, which simulated the anisotropic soil strength as depicted in Figure 35, predicted failure at an embankment height of 3.9m, which is the failure height observed on site. For the same embankment, but now analysed with the MCC model with an isotropic undrained strength corresponding to the triaxial compression profile in Figure 35, the failure height is grossly overestimated at 4.9m. Back analysis using the MCC model to achieve a failure height of 3.9m with an isotropic strength resulted in the necessary strength being 1.25 times the DSS strength. Analysis with the isotropic strength being equal to the DSS profile, which is what some design practice suggests, is largely conservative, predicting failure at only 3.3m embankment height.

A further set of analyses was performed, where the embankment geometry was altered to have berms on both sides of the embankment, see insert in Figure 37. Again both anisotropic and isotropic analyses were performed and the results are presented in Figure 37, as normalised horizontal displacement of the embankment toe versus embankment height.

An analysis using the MIT-E3 model predicted that, with the help of a berm, the embankment could now be erected to 4.4m. The same embankment was then analysed with the MCC model, with the isotropic strength back-calculated from the previous set of analyses (i.e. 1.25 times the DSS strength, see Figure 36). This analysis predicted an embankment height at failure of 4.9m and therefore overestimated that obtained by the analysis with the MIT-E3 model. To obtain the same failure height as the MIT-E3 analysis, the MCC analysis needed a strength of only 1.15 times the DSS strength.

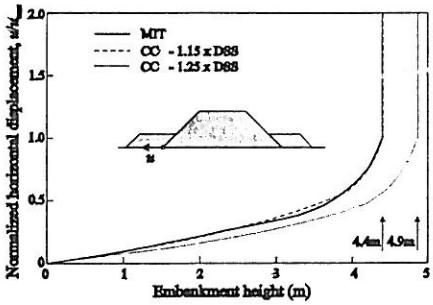

Figure 37: Failure of Saint-Alban embankment - modified geometry

Several conclusions can be drawn from this embankment study:

- Analysis which assumes isotropic soil behaviour and takes either the triaxial compression strength profile or the DSS strength profile will either overestimate or underestimate the embankment height at failure, respectively;
- Taking account of soil anisotropy, observed through laboratory and field experiments, enables a more accurate prediction of embankment height at failure;
- If an isotropic strength profile is back-calculated from the observed behaviour of a certain embankment geometry, it is not necessarily appropriate if the embankment geometry becomes slightly altered.

Clearly in the future, as more experimental data becomes available, and user friendly constitutive models are developed, it will be possible to model anisotropic behaviour in most field problems. At present, the necessary laboratory test data is rarely available and even if it were, the determination of the model parameters is not straight forward.

8 CONCLUSIONS

The examples given in this paper demonstrate that care must be exercised when choosing a constitutive model for carrying out geotechnical analysis. In particular, it has been shown that the small strain behaviour and whether or not this involves purely elastic or a combination of elastic and plastic strains can have significant effects on the accuracy of any predictions.

There are many constitutive models available for the analysis of geotechnical problems, but there are no universally applicable models. Pre-failure models that perform well for some situations do not perform well for others, although some models have wider application than others. It is therefore important for the analyst to consider which issues and facets of soil behaviour are likely to dominate and then choose a model accordingly. In the case of the Saint- Alban embankment, anisotropy was important, but for other problems perfectly reasonable predictions were made without considering it.

It is pointless using a model which will predict settlements accurately when lateral movements are an issue. Likewise, certain models may predict the behaviour of a structure reasonably well, but they do not predict remote movements well and so potential damage of remote structures and/or services is underpredicted. Problems where stress changes occur on a boundary which is remote from the point of interest present a real challenge (e.g. tunnels) and it is generally necessary to use sophisticated constitutive models for the analysis of this class of problem.

Not withstanding the above difficulties, it has been shown that, with experience and the appropriate software, it is possible to make accurate Class A predictions (before the event).

ACKNOWLEDGEMENTS

The author would like to thank Mr K. Higgins and Dr N. Kovacevic of the Geotechnical Consulting Group and Dr L. Zdravkovic from Imperial College for their contributions to some of the case histories discussed in this paper.

REFERENCES

Addenbrooke, T.I., Potts, D.M. & Puzrin, A.M. 1997. The influence of pre-failure soil stiffness on the numerical analysis of tunnel construction. *Geotechnique* 47, 3: 693-712.

Connolly T.M.M. 2002. The geological and geotechnical properties of a glacial lacustrine clayey silt, PhD thesis in preparation, Imperial College, University of London.

Coop M.R. 1990. The mechanics of uncemented carbonate sands, *Geotechnique* 40, 4: 607-626.

Cotecchia F. 1996. The effects of structure on the properties of an Italian pleistocene clay. PhD thesis, Imperial College, University of London.

Fernie, R., Kingston, P.J., St John, H.D., Higgins, K.G. & Potts, D.M. 1996. Case history of a "stepped box" excavation in soft ground at the sea front, Langley Point, Eastbourne. *Geotechnical Aspects of Underground Construction in Soft Clay*, R.J. Mair & R.N. Taylor (Eds): 123-130. Rotterdam: Balkema.

Hight D.W. 1998. Soil characterisation: the importance of structure, anisotropy and natural variability, 38th Rankine lecture, *Geotechnique*, in preparation.

Jardine, R.J. & Potts, D.M. 1988. Hutton tension leg platform foundations: prediction of driven pile behaviour. *Geotechnique* 38, 2: 231-252.

Jardine, R.J., Hight D.W. & McIntosh W. 1988. Hutton tension leg platform foundations: measurement of pile axial load-displacement relations. *Geotechnique* 38, 2: 219-230.

Kohata Y., Tatsuoka F., Wang L., Jiang G.L., Hoque E. & Kodaka T. 1997. Modelling of nonlinear deformation properties of stiff geomaterials, *Geotechnique* 47, 3: 563-580.

La Rochelle, P., Trak, B., Tavenas, F.A. & Roy, M. 1974. Failure of a test embankment on a sensitive Champlain clay deposit. *Canadian Geotechnical Journal* 11: 142-164.

Lade P.V. & Duncan J.M., 1975. Elasto-plastic stress-strain theory for cohesionless soil, *ASCE, GT Div.*, 101, 1037-1053.

Matsuoka H. & Nakai T. 1974. Stress-deformation and strength characteristics of soil under three different principal stresses, *Proc. Jap. Sic. Civ. Eng.*, 232, 59-70.

Nyren, R. 1998. Field measurements above twin tunnels in London Clay. *PhD thesis*, Imperial College, University of London.

Ochiai H. & Lade P.V. 1983. Three-dimensional behaviour of sand with anisotropic fabric, *ASCE, GT Div.*109, 10: 1313-1328.

Pestana J.M. 1994. A unified constitutive model for clays and sands, PhD thesis, Massachusetts Institute of Technology, Cambridge, USA.

Potts, D.M., Dounias, G.T. & Vaughan P.R. 1990. Finite element analysis of progressive failure of Carsington embankment. *Geotechnique* 40, 1: 79-101.

Potts, D.M. & Zdravkovic, L. 1999. *Finite element analysis in geotechnical engineering: Theory*. London: Thomas Telford.

Potts, D.M. & Zdravkovic, L. 2001. *Finite element analysis in geotechnical engineering: Applications*. London: Thomas Telford.

Roscoe K.H. & Burland J.B.1968 On the generalised

stress-strain behaviour of 'wet' clay, *Eng. Plasticity*, Cambridge Univ. Press, 535-609.

Sarrailh, J. & Tavenas, F.A. 1972. Etude geotechnique preliminarie du site de Saint-Alban. *Internal report GCN-72-09-02 (MS-N2)*. University of Laval, Quebec, Canada.

Seah T.H. 1990. Anisotropy of normally consolidated Boston Blue clay, ScD thesis, Massachusetts Institute of Technology, Cambridge, USA.

Smith P.R. 1992 . The behaviour of natural high compressibility clay with special reference to construction on soft ground, PhD thesis, Imperial College, University of London.

Soga K., Nakagawa K. & Mitchel J.K. 1995. Measurement of stiffness degradation characteristics of clay using a torsional shear device, Earthquake geotechnical engineering, IS-Tokyo, Edt. K. Ishihara, Balkema, 1: 107-112.

Standing, J.R., Farina, M. & Potts, D.M. 1998. The prediction of tunnelling indiced building settlements - a case study. *Tunnels & Metropolises*, A. Negro & A.A. Ferreira (Eds): 1053-1058. Rotterdam: Balkema.

Tavenas, F.A. & Chapeau, C. (1973). Etude en laboratorie des proprietes geotechniques de largile de Saint-Alban. *Internal report GCN-73-04-03 (MS-N5)*. University of Laval, Quebec, Canada.

Whittle, A.W. 1993. Evaluation of a constitutive model for overconsolidated clays. *Geotechnique*, 43, 2:289-314.

Wilson, A.C. & Evans, J.D. 1990. The use of low grade rockfill at Roadford Dam. *The Embankment Dam*. London: Thomas Telford: 15-21.

Zdravkovic, L., Potts, D.M. & Hight, D.W. 2002. The effect of anisotropy on the behaviour of an embankment on soft ground. *Geotechnique* 52, 6: 447-457.